

# Anomalous enhanced Raman scattering from longitudinal optical phonons on Ag-nanoparticle-covered GaN and ZnO

C. Y. Liu,<sup>1,a)</sup> M. M. Dvoynenko,<sup>2</sup> M. Y. Lai,<sup>2</sup> T. H. Chan,<sup>2,3</sup> Y. R. Lee,<sup>2</sup> J.-K. Wang,<sup>2,4,b)</sup> and Y. L. Wang<sup>2,5,c)</sup>

<sup>1</sup>Department of Electro-Optical Engineering, National Cheng Kung University, Tainan 70101, Taiwan

<sup>2</sup>Institute of Atomic and Molecular Sciences, Academia Sinica, P.O. Box 23-166, Taipei 10617, Taiwan

<sup>3</sup>Department of Chemistry, National Taiwan University, Taipei 10617, Taiwan

<sup>4</sup>Center for Condensed Matter Sciences, National Taiwan University, Taipei 10617, Taiwan

<sup>5</sup>Department of Physics, National Taiwan University, Taipei 10617, Taiwan

(Received 20 August 2009; accepted 25 November 2009; published online 20 January 2010)

The authors report experimental studies of surface-enhanced Raman scattering (SERS) of wurtzite-type GaN and ZnO crystalline samples covered with Ag-nanoparticles. The longitudinal optical phonons consistently exhibit unusually intense Raman enhancement in comparison with other phonons. The anomaly is interpreted by a proposed model based on a resonant Raman scattering process assisted by metal-induced gap states at the Ag/GaN and Ag/ZnO interfaces. This study suggests that SERS of lattice vibrations in inorganic semiconductors is sensitive to their propagation nature, providing a progressive perspective view on electron-mediated enhanced Raman scattering. © 2010 American Institute of Physics. [doi:10.1063/1.3291041]

Surface-enhanced Raman scattering (SERS) has attracted attention in the past three decades, because it allows the use of Raman scattering to detect small quantity of chemicals and biomolecules.<sup>1</sup> Owing to the recent progresses in nanofabrication, SERS substrates with uniformly high Raman enhancement has been realized.<sup>2</sup> Understanding and controlling the two enhancement mechanisms of SERS, i.e., electromagnetic and chemical enhancements, are among the most important issues concerning its further development. The former originates from the local field enhancement created by electromagnetic resonance (plasmon) in the proximity of Ag nanoparticles at the excitation wavelength as well as the increased emission at Raman-shifted wavelengths owing to enhanced local photon density of states.<sup>3</sup> The chemical enhancement alternatively stems from photon-induced dynamic electron transfer between a molecule and its proximal metallic nanostructure. Experimental methods have been proposed to determine the enhancement factors of these two mechanisms separately.<sup>4</sup> Although several theoretical models have been proposed to understand the nature of chemical enhancement,<sup>5</sup> experimental verification lags behind. The main reason lies in our extremely poor control of molecular adhesion on metal nanostructures that serve as Raman enhancer.

In comparison with molecular species, semiconductors can benefit the investigation of the chemical enhancement for the following three advantages. First, the electron and phonon systems of semiconductors are relatively simple and well understood. Second, the controllable metal-semiconductor interface can be easily prepared in a clean environment and can be characterized experimentally. Third, the interrogation is supported by many former research efforts at the metal-semiconductor interfaces. Although a few works have demonstrated SERS of semiconductor materials,<sup>6</sup>

no systematic study has been carried out so far. Here, we present experimental results of SERS of GaN and ZnO crystalline systems, hoping to shed some lights on the mechanism of chemical enhancement.

Two kinds of wurtzite-type crystals were used in the study as follows: (1) *n*-type *c*- and *a*-plane GaN epitaxial films and (2) single-crystal *n*-type *c*- and *m*-plane ZnO wafers. The 500 nm *c*-plane GaN film was grown on a 6H-SiC substrate by chemical vapor deposition, while the 900 nm *a*-plane one was grown on a sapphire substrate by the same method. Each sample was partially covered with Ag nanoparticles (particle size of 10–40 nm) by thermal deposition at a rate of 0.3 Å/s, yielding an average thickness of 5 nm for the ZnO samples and of 10 nm for the GaN samples. The Ag-covered and pristine areas were used for SERS and normal Raman measurements in air, respectively. The excitation light source for the GaN samples was a continuous-wave frequency-doubled Nd:YAG laser emitting at 532 nm, while that for the ZnO samples was a HeCd laser emitting at 325 nm. Because the absorption coefficient of ZnO at 325 nm is  $1.7 \times 10^5 \text{ cm}^{-1}$ ,<sup>7</sup> its Raman signal comes from the top 60 nm layer, greatly reducing the bulk contribution. The Raman radiation, collected in the backward direction, was sent through a notch filter, and then to a monochromator for spectral analysis. The dispersed spectra were detected by a liquid-nitrogen cooled charge-coupled device. A calibration procedure gave a spectral resolution of  $<7 \text{ cm}^{-1}$  and a Raman-shift error of  $<0.1 \text{ cm}^{-1}$ . For each sample, the SERS and Raman measurements were performed under the same condition. The measurement geometry is described as  $k_i(e_i, e_s)k_s$ , where  $k_i$  ( $k_s$ ) is the incident (scattered) light direction, while  $e_i$  ( $e_s$ ) is the corresponding polarization direction. The *c*-axis of the samples is assigned to *Z*-axis while *X*- and *Y*-axis, perpendicular to each other, are arbitrarily selected from a plane perpendicular to *Z*-axis.

A hexagonal wurtzite crystal has four Raman active optical phonon modes:  $A_1$ ,  $E_1$ , and two  $E_2$ . Each of the  $A_1$  and  $E_1$  modes splits into longitudinal optical (LO) and transverse

<sup>a)</sup>Electronic mail: chihiliu@mail.ncku.edu.tw.

<sup>b)</sup>Electronic mail: jkwang@ntu.edu.tw.

<sup>c)</sup>Electronic mail: ylwang@pub.iam.s.sinica.edu.tw.

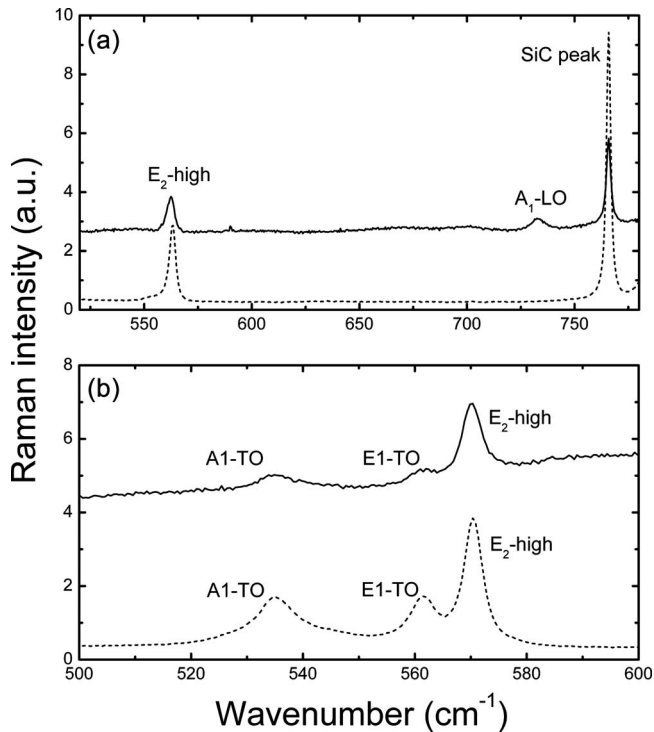


FIG. 1. SERS (solid lines) and Raman scattering (dotted lines) spectra of (a) *c*-plane GaN epitaxial film in  $Z(-,-)\bar{Z}$  geometry and (b) *a*-plane GaN epitaxial film in  $X(-,-)\bar{X}$  geometry. The SERS spectra are up-shifted relative to the Raman spectra for clearance.

optical (TO) modes. The two  $E_2$  modes are, respectively, named as  $E_2$ -high and  $E_2$ -low modes according to their vibrational frequencies. Owing to their symmetry-sensitive dependences, only some of the optical modes are observable in a specific Raman geometry. Figure 1(a) shows the Raman and SERS spectra of the *c*-plane GaN film in  $Z(-,-)\bar{Z}$  geometry, where “-” denotes a nonpolarized condition. The prominent peak at  $563\text{ cm}^{-1}$  in the Raman spectrum is assigned to the  $E_2$ -high mode.<sup>8</sup> The expected Raman peak at  $732\text{ cm}^{-1}$  ( $A_1$ -LO mode) is probably submerged in the tail of the nearby huge peak at  $767\text{ cm}^{-1}$  from the  $E_2$  mode of the SiC substrate. In contrast, the SERS spectrum clearly shows the  $A_1$ -LO peak, indicating that the Raman enhancement effect occurs at this mode. On the other hand, the  $E_2$ -high peak in the SERS spectrum is weaker than that in the Raman spectrum, probably due to the obstruction by the covered Ag nanoparticles. The obstruction induces a peak reduction of 68% by comparing the background SiC peaks of  $767\text{ cm}^{-1}$  in the two spectra. However, the  $E_2$ -high peak is reduced by 52%, indicating the occurrence of Raman enhancement but its enhancing factor much smaller than the  $A_1$ -LO’s one. For comparison, Fig. 1(b) shows the Raman and SERS spectra of the *a*-plane GaN film in  $X(-,-)\bar{X}$  geometry. Consistent with the previous work,<sup>9</sup> three prominent peaks emerge at  $570\text{ cm}^{-1}$  ( $E_2$ -high),  $561\text{ cm}^{-1}$  ( $E_1$ -TO), and  $535\text{ cm}^{-1}$  ( $A_1$ -TO). Their SERS signals, being weaker than the corresponding Raman ones, similarly exhibit much weaker enhancement than the  $A_1$ -LO peak.

Figure 2(a) shows the Raman and the SERS spectra of *c*-plane ZnO crystal in  $Z(-,-)\bar{Z}$  geometry. Two peaks emerge at  $438\text{ cm}^{-1}$  ( $E_2$ -high) and  $575\text{ cm}^{-1}$  ( $A_1$ -LO) in the normal Raman spectrum.<sup>8</sup> Similar to the result of GaN, the

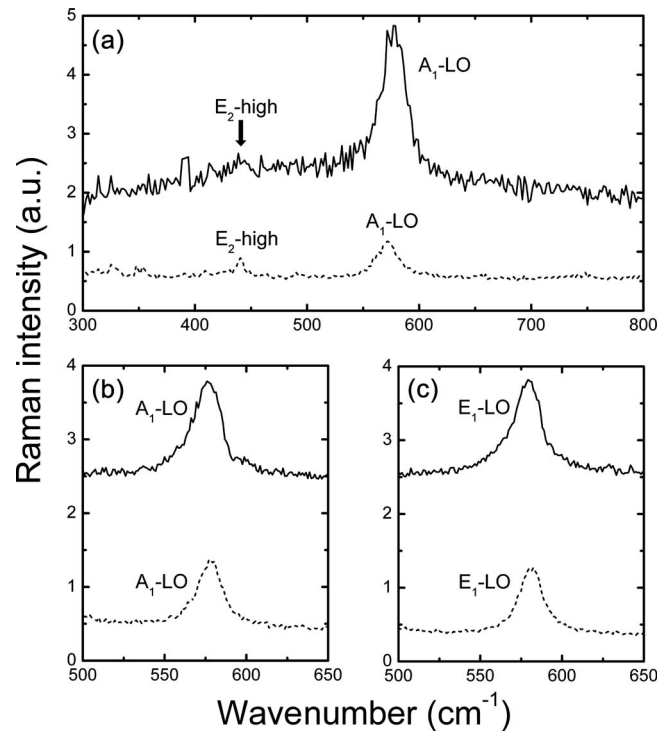


FIG. 2. SERS (solid lines) and Raman scattering (dotted lines) spectra of (a) *c*-plane ZnO crystal in  $Z(-,-)\bar{Z}$  geometry and *m*-plane ZnO crystal in (b)  $X(Z,Z)\bar{X}$  and (c)  $X(Y,Y)\bar{X}$  geometries. The SERS spectra are up-shifted relative to the Raman spectra for clearance.

SERS signal of the  $A_1$ -LO peak is about three times of the Raman signal, while the SERS signal of the  $E_2$ -high peak is almost diminished. In comparison, the SERS signals of the *m*-plane ZnO sample that was used to observe the  $A_1$ -LO and  $E_1$ -LO modes are consistently higher than their corresponding Raman signals, as shown in Figs. 2(b) and 2(c). Combining the measurements of the GaN and ZnO samples, we then conclude that the SERS enhancement for the LO phonon modes are higher than that for the non-LO ones. This conclusion suggests that the SERS enhancement factor in crystalline semiconductors is sensitive to the phonon propagation direction.

Can we understand the observed anomalous enhancement within the framework of the existing SERS mechanisms: electromagnetic and chemical enhancement? Because of the relatively weak wavelength dependence of the electromagnetic enhancement mechanism for nonuniform Ag nanoparticles, it endows all the phonon modes with similar enhancement factor. If electrons take part in the SERS process as suggested in the chemical enhancement mechanism, the nature of the electron-phonon (e-p) interaction must play an essential role in producing this LO-phonon-specific effect. According to a theoretical study by Chen and co-workers,<sup>10</sup> the e-p interaction of TO mode is two orders of magnitude smaller than that of the LO mode for ZnO or GaN, while that of the  $E_2$ -high mode is even smaller. As a result, only the LO modes produce significant e-p interaction in the wurtzite crystals.

If e-p interaction is indeed the origin of the observed anomaly, the following question naturally emerges: what is the source of these free electrons. Since the photon energy of the 532 nm laser (2.3 eV) is below the band gap of GaN (3.4 eV), the generation of free electrons in the conduction

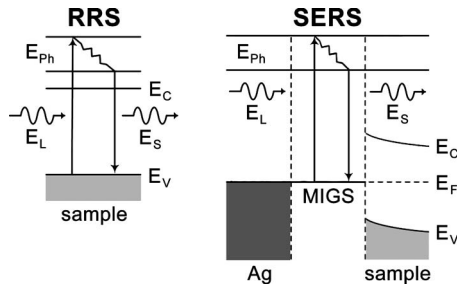


FIG. 3. Proposed schematics of RRS and SERS processes on crystalline semiconductors. MIGS stands for metal-induced gap states.  $E_L$  ( $E_S$ ) represents the photon energy of the excitation laser (the Stokes radiation);  $E_C$  ( $E_V$ ) is the energy of the conduction band minimum (the valence band maximum);  $E_F$  ( $E_{Ph}$ ) denotes the Fermi energy (the phonon energy).

band is inhibited. We therefore propose that some gap states formed at the metal-semiconductor interface, so called metal-induced gap states (MIGS), likely to be candidates for the source of electrons. Theoretical calculation by Picozzi and co-workers<sup>11</sup> showed that MIGS are formed at the Ag/GaN interface just in proximity to the Fermi energy. This result suggests that considerable electron occupation in equilibrium may reside in the MIGS and meanwhile the Schottky barrier at the semiconductor side can be developed to maintain charge neutrality. Because the Schottky barrier is  $\sim 0.8$  eV (Ref. 12) for the Ag/GaN interface and  $\sim 0.9$  eV (Ref. 13) for Ag/ZnO interface, the incident laser can promote the electrons in the occupied MIGS to resonate with specific unoccupied electronic states in the conduction bands of GaN and ZnO. The presence of MIGS may thus provide the starting states for a resonant Raman scattering (RRS) process. We therefore propose a MIGS-assisted RRS process, sketched in Fig. 3, to explain the observed anomalous SERS enhancement of LO modes. An occupied electron in the MIGS is excited by the locally enhanced optical field to the conduction band. Similar to RRS, the excited electron is then scattered to another state in the conduction band through e-p interaction. This is followed by the emission of a Raman photon through the recombination of the electron with the hole left in the MIGS. The prominent electron-LO phonon interaction, as described above, can thus enhance the Raman scattering. This MIGS-assisted RRS process works with the resonant electromagnetic interaction with Ag nanoparticles to yield the final enhanced Raman scattered radiation.

We note that a recent work on a *c*-plane GaN thin film in a tip-enhanced Raman scattering (TERS) scheme shows only significant Raman enhancement on the  $E_1$ -TO mode, instead of the  $A_1$ -LO mode,<sup>6</sup> which seems contrary to our observation. This inconsistency can be explained by the fact that the near-field polarization at the tip apex is along the tip axis and therefore the *c*-axis of the sample, forbidding the excitation of the LO-phonon modes. In contrast, the near-field polarization around individual Ag nanoparticles is preferably parallel to the sample surface, similar to the pristine area, making the comparison between the Raman and the SERS experimental results simpler. Finally, for diamond, silicon, and germanium, the nonionic structure creates negligible e-p interaction, resulting in the absence of the anomalous SERS enhancement. However, strain or structural defects within these semiconductor systems may create nonzero local dipole field to revive the e-p scattering mechanism in the SERS process. This prediction is consistent with the observation of local strain with TERS.<sup>14</sup> SERS therefore represents a potential technique to probe local strain and defects.

The authors thank the instrumental support by Center of EMO Materials and Nanotechnology in National Taipei University of Technology and Mr. Chi-Feng Lin for preparing some samples. This work is supported by National Science Council (Grant No. NSC 96-2120-M-001-002) and Academia Sinica in Taiwan.

- <sup>1</sup>K. Kneipp, M. Moskovits, and H. Kneipp, *Surface-Enhanced Raman Scattering: Physics and Application* (Springer, Berlin, 2006).
- <sup>2</sup>H.-H. Wang, C.-Y. Liu, S.-B. Wu, N.-W. Liu, C.-Y. Peng, T.-H. Chan, C. F. Hsu, J.-K. Wang, and Y.-L. Wang, *Adv. Mater.* **18**, 491 (2006).
- <sup>3</sup>S. V. Gaponenko and D. V. Guzатов, *Chem. Phys. Lett.* **477**, 411 (2009).
- <sup>4</sup>M. M. Dvovnyenko and J.-K. Wang, *Opt. Lett.* **32**, 3552 (2007).
- <sup>5</sup>A. Otto, *J. Raman Spectrosc.* **36**, 497 (2005).
- <sup>6</sup>R. Matsui, P. Verma, T. Ichimura, Y. Inouye, and S. Kawata, *Appl. Phys. Lett.* **90**, 061906 (2007).
- <sup>7</sup>P. L. Washington, H. C. Ong, J. Y. Dai, and R. P. H. Chang, *Appl. Phys. Lett.* **72**, 3261 (1998).
- <sup>8</sup>M. A. Stroscio and M. Dutta, *Phonons in Nanostructures* (Cambridge University Press, Cambridge, 2001).
- <sup>9</sup>T. Azuhata, T. Soat, K. Suzuki, and S. Nakamura, *J. Phys.: Condens. Matter* **7**, L129 (1995).
- <sup>10</sup>C. Chen, M. Dutta, and M. A. Stroscio, *Phys. Rev. B* **70**, 075316 (2004).
- <sup>11</sup>S. Picozzi, A. Continenza, G. Satta, S. Massidda, and A. J. Freeman, *Phys. Rev. B* **61**, 16736 (2000).
- <sup>12</sup>T. U. Kampen and W. Mönch, *Appl. Surf. Sci.* **117**, 388 (1997).
- <sup>13</sup>Y. Dong and L. J. Brillson, *J. Electron. Mater.* **37**, 743 (2008).
- <sup>14</sup>Y. Saito, M. Motohashi, N. Hayazawa, M. Iyoki, and S. Kawata, *Appl. Phys. Lett.* **88**, 143109 (2006).